Received: 21 September 2021 | Revised: 3 February 2022 | Accepted: 22 March 2022

DOI: 10.1002/elps.202100311

ELECTROPHORESIS

RESEARCH ARTICLE

A compact microfluidic geometry for multiplexing enzyme-linked immunosorbent assays

Basant Giri | **Debashis Dutta**

Department of Chemistry, University of Wyoming, Laramie, Wyoming, USA

Correspondence
Debashis Dutta, Department of Chemistry, (Dept. # 3838), University of Wyoming, 1000 East University Avenue, Laramie, WY 82071, USA.
Email: ddutta@uwyo.edu

Color online: See article online to view Figures 1–5 in color.

Abstract

We have previously reported a novel approach to implementing multiplex enzyme-linked immunosorbent assay (ELISA) in connected microchannels by exploiting the slow diffusion of the enzyme reaction product across the different assay segments. This work builds on that report by implementing the noted assay in segments arranged along the circumference of a circular channel layout to reduce the footprint size and sample volume requirement. Using the current design, a 5-plex cytokine ELISA was demonstrated in a 1.5 × 1.5-cm region, which corresponded to a reduction in the footprint area by about a factor of 3 compared to that reported in our previous study. Additionally, the selective coating of our assay segments with the target molecules was realized in this work using electroosmosis instead of hydrodynamic flow as was the case in the previous report. This aspect of our experimental design is particularly significant as it permits the use of cross-sectional channel dimensions significantly shorter than those employed in the current work. Moreover, the use of an electric field for coating purposes enables the integration of functionalities such as electrokinetic preconcentration of analyte molecules during the sample incubation period that can further enhance the capabilities of our assay method.

KEYWORDS

diffusion, electroosmotic flow, ELISA, microfluidic, multiplex

1 | INTRODUCTION

Enzyme-linked immunosorbent assay (ELISA) offers a highly specific and sensitive approach for quantitating a variety of chemical and biological analytes in complex matrices [1, 2]. The high specificity of the ELISA method originates from its reliance on antibody–antigen interactions dictated by the specific chemical constitution of the species involved and the environment they interact in. The high sensitivity of the assay on the other hand arises from signal amplification by an enzyme label bound to the immuno-complex immobilized on a solid surface. In addition, the implementation of this assay is relatively simple and typically involves only a series of washing and incubation steps prior to the final quantitation, using a variety of detection methods [3, 4]. Not surprisingly, ELISA is widely accepted as a gold standard for quantitating any analyte to which an antibody can be generated and has been successfully applied to samples relevant to biological research, biomedical testing, environmental monitoring and food assessment applications among others [5–8]. Over the years, significant improvements in the performance of ELISA methods have been reported through efficient immobilization of the target analyte on an assay surface and/or minimization of nonspecific binding to it [9], development of high performance enzyme label-substrate

couples [10, 11] and construction of sensitive detection systems [12]. More recently, this immunoassay has been demonstrated on inexpensive paper-based devices [13, 14] and integrated to detection platforms that are easily accessible and require minimal training to operate [15, 16].

It is being increasingly recognized that in order to comprehensively understand the behavior of complex real-world systems, highly sensitive assays with the ability to simultaneously quantitate a group of molecular signatures are desirable. In this regard, there has been a concerted effort over the past two decades to enable multiplex ELISAs that are capable of reliably detecting a small number of analyte molecules. A variety of miniaturized assay platforms have been reported to realize this capability with analyte detection limits down to a single molecule [17–19]. These platforms have typically relied on the large signal-to-noise ratio in their measurements as well as on the spatial isolation of individual analyte particles to realize the desired detection limit. However, the operation and maintenance of these systems are often complicated making them difficult to adopt by biological researchers. Additionally, their integration to commercially available readout devices, for example, microplate readers, tends to be challenging requiring them to rely on specialized instrumentation for support. As a result, these platforms can be quite demanding for a vast number of researchers interested in making measurements with sample volumes in the range of 10 µl to 10 nl but not necessarily at the single molecule level.

To cater to the needs of this group of researchers, we have previously reported on a microfluidic device capable of performing multiplex ELISAs using sample volumes in the desired range in a relatively simple fashion [20]. In the reported device, different analytes were quantitated in a single microfluidic channel by exploiting the slow diffusion of the enzyme reaction product across the different assay segments. A linear array of ELISA regions were created within a straight conduit by selectively patterning them with the chosen antibodies/antigens via a flow-based method. The different analytes were then captured in their respective assay segments by incubating a 5-µl aliquot of the sample in the analysis channel for a prescribed amount of time. Once the ELISA surfaces have been prepared and the enzyme substrate introduced into the analysis channel, it was observed that the concentration of the enzyme reaction product (resorufin) at the center of each assay region grew linearly with time. Further, the rate of resorufin generation at these locations was found to be proportional to the concentration of the analyte being assayed in that segment provided that the enzyme reaction time was kept much shorter than that required by the resorufin molecules to diffuse across the different assay segments. Under these operating conditions, the reported device was shown to yield a limit of detection for the target analyte concentration similar to that realized on commercial microwell plates but using only about a 20th of the sample volume.

In the present work, we build on our previous report by implementing multiplex ELISAs in segments arranged along the circumference of a circular channel layout to reduce the footprint size and sample volume requirement. The noted approach enabled us to perform a 5-plex cytokine assay in a 1.5 cm × 1.5-cm region that corresponded to a reduction in the footprint area by about a factor of 3 compared to that reported in our previous study. Additionally, the selective coating of the assay segments with the target molecules was realized in this work using electroosmotic transport instead of hydrodynamic flow as was the case in the previous study. This aspect of our experimental design is particularly significant as it permits the use of cross-sectional channel dimensions significantly shorter than those employed in this work. Moreover, the use of an electric field for coating purposes enables the integration of functionalities such as the electrokinetic preconcentration of analyte molecules during the sample incubation period that can further enhance the capabilities of our assay method.

2 | MATERIALS AND METHODS

2.1 | Device fabrication

For fabricating the microfluidic devices employed in this work, bottom substrates and cover plates made from borosilicate glass were purchased from Telic Company (Valencia, CA). Although the purchased cover plates had both their faces unprotected, the bottom substrates came with a thin layer of chromium and photoresist laid down on one of their surfaces. The fabrication process for the microchips was initiated by photolithographically patterning [21, 22] the desired channel layout (see Figure 1A) on the bottom substrate using a custom-designed photomask created through Fineline Imaging Inc. (Colorado Springs, CO). The channel width in our device was chosen to be 500 µm for the entire microfluidic network with five assay segments (marked A–E in Figure 1A) created along the circumference of a circular channel layout having an outer diameter of 9 mm. The length of each assay segment in this situation was about 5.65 mm along their outer edge. Auxiliary channels were also created emanating from the outer and inner edges of our circular channel layout to allow the introduction of reagents from liquid reservoirs (marked 1–6 in Figure 1A) into the assay segments as needed. The liquid reservoirs in this design were placed at the terminals of the auxiliary channels. After completion of the

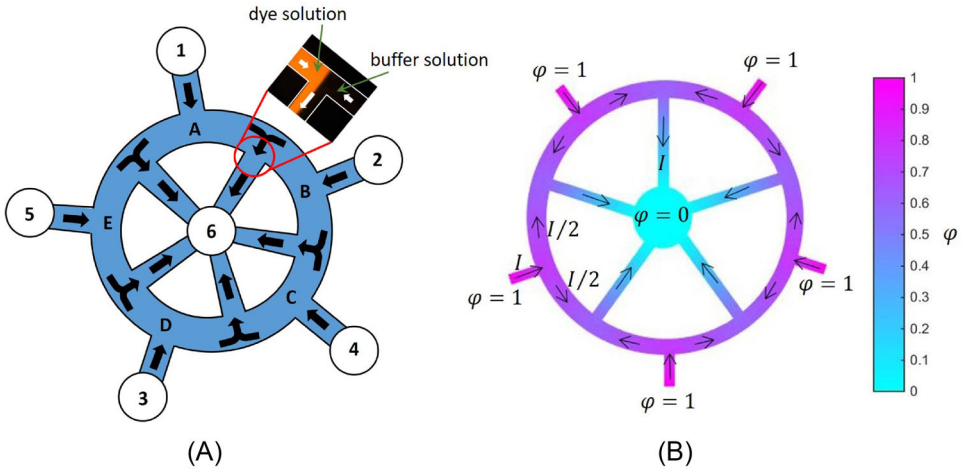

FIGURE 1 (A) Schematic of the microchip device employed in the present work. The arrows in the figure indicate the direction of electroosmotic flow during selective patterning of the different assay segments. The subfigure also includes a fluorescent image showing the electroosmotic flow of a dye solution (10-μM rhodamine B prepared in 10-mM sodium phosphate buffer, pH 7.2) from segment A and the dye-free buffer from segment B upon applying 50 V across the upstream (ports 1–5) and downstream (port 6) liquid reservoirs. (B) Numerical simulation of the electric voltage distribution in the fluidic network upon applying 1 V at the upstream reservoirs and electrically grounding the downstream one. These simulations predict the electrical current (I), electric field and therefore the EOF in the straight channel segments to be twice their magnitudes in the curved regions. EOF, electroosmotic flow

photopatterning process, the photoresist layer was cured in microposit developer MF-319 (Rohm and Haas) and the chromium layer removed along the channel network with a chromium etchant (Transene Inc.). The channels were then etched to a chosen depth of 30 μm using a solution of buffered oxide etchant purchased from Transene Inc. Access holes were drilled at the channel terminals using a microabrasive powder blasting system (Vaniman Inc.) to allow the introduction of liquid reagents/sample into the microchannels. Finally, the microfluidic network was sealed off by bringing a cover plate in contact with the bottom substrate in deionized water and then allowing the two plates to bond under ambient conditions overnight [23, 24]. Cylindrical glass reservoirs with internal volumes of about 150 μl were affixed over the access holes using an ultraviolet light-curable glue (Norland Products Inc.) to serve as a source or sink for the liquid flow within the microchannels.

2.2 | Device preparation

The microchip device thus fabricated was prepared for an experiment by first rinsing its conduits with 1-M sodium hydroxide (Sigma-Aldrich) for 1 h and then with deionized water for 10 min. These channels were later dried at 80°C in a forced-air convection oven before treating them with a solution of (3-aminopropyl)triethoxysilane (Sigma-Aldrich) for an hour under ambient conditions. Subsequently, the fluidic network was rinsed with methanol and then reacted at room temperature with an aqueous solution containing 5% w/v glutaraldehyde (Sigma-Aldrich) for another 60 min to create a surface that could be covalently bonded to the amine groups on a protein molecule. Finally, excess glutaraldehyde was removed from the system by rinsing the microchip with deionized water for about 5 min. Note that in all of the rinsing and coating steps described previously, the reagents were introduced into reservoirs 1–5 with vacuum applied at reservoir 6. Although vacuum was applied for the entire period during the rinsing steps, the coating process involved the application of vacuum for only about 5 s following which reservoir 6 was maintained at ambient pressure for the rest of the coating period. The flow introduced during both the rinsing and coating steps allowed uniform distribution of the reagents into the entire fluidic network to ensure a homogenous treatment of all channel surfaces.

Following the derivatization of the channel surface with glutaraldehyde, distinct assay regions were created in segments A–E by treating them with solutions containing different concentrations/kinds of reagents. For example, in order to obtain the calibration curves for our cytokine sample containing human TNF-α, IL-1α, IL-4, IL-6 and IFN-γ, the microchip was prepared by coating its different assay segments with solutions containing different concentrations of the respective cytokine. Specifically, the calibration device for each cytokine was realized by first incubating a 5-μg/ml solution of the respective capture antibody (BD Biosciences) prepared in a 0.1-M carbonate–bicarbonate buffer (pH 9.4) in the entire microfluidic network for 1 h.

This step was followed by a 10-min rinse with a 0.1-M phosphate buffer (pH 7.2) and then 1-h incubation with a solution of 1% (w/v) bovine serum albumin (BSA) prepared in the carbonate–bicarbonate buffer to block off the remaining reactive sites on the channel surface. The excess BSA was subsequently rinsed out with the phosphate buffer and the different assay segments then coated with different concentrations of the chosen cytokine sample. A sample diluent provided by the vendor (BD Biosciences) was used to produce different dilutions of the chosen cytokine species. To realize this coating step, the cytokine solutions were placed in reservoirs 1–5 in the order of increasing concentration and slowly transported via electroosmosis into reservoir 6 to prevent their diffusive mixing within the fluidic network during the coating period. Electroosmotic flow (EOF) is produced upon subjecting an electrolyte in contact with an electrically charged solid surface to an external electric field [25]. The flow occurs as the nonneutral electrical double layer formed at the solid–fluid interface under these conditions experiences a body force dragging the bulk liquid with it. EOF has been reported around immunoassay surfaces although its magnitude and/or direction are known to be altered during the surface preparation process [26, 27]. This alteration in EOF velocity results from a change in the amount of electrical charge on the assay surface upon its derivatization and attachment to the relevant macromolecules. Previous research in our group has shown that when glass channels are prepared for an immunoassay, the direction of EOF does not change but its magnitude is reduced [28, 29]. The same behavior was observed in our present work with glass devices yielding EOF from the high voltage to the low voltage end of the channel. In this situation, the flow pattern shown in Figure 1A needed to react the different segments of our fluidic network with different cytokine concentrations was realized by applying 50 V to reservoirs 1–5 while electrically grounding reservoir 6. The noted voltage was chosen as it maintained sufficient EOF to prevent diffusive mixing in the fluidic network without drawing more than 10 µl of the cytokine solution from reservoirs 1–6 during the 1-h coating period. After immobilizing the cytokine molecules, the entire fluidic network was again rinsed with the phosphate buffer and later coated with the biotinylated detection antibody solution for 1 h. The excess antibodies were then removed with a phosphate buffer wash followed by the treatment of all the channel segments with a 0.2-µg/ml solution of streptavidin-conjugated alkaline phosphatase for another 1 h to complete the assay surface.

To prepare a multiplex device, we followed a similar procedure to that described earlier except for modifying the capture antibody and sample incubation steps. For this device, the five assay segments were coated with five different capture antibodies relevant to our cytokine sample by placing those solutions in reservoirs 1–5. The 5-µg/ml antibody solutions prepared in the 0.1-M carbonate–bicarbonate buffer were then slowly transported via electroosmosis into reservoir 6 applying 50 V to reservoirs 1–5 while electrically grounding reservoir 6 for 1 h. After washing the excess antibodies with phosphate buffer and capping off the remaining reactive sites with 1% (w/v) BSA, the sample containing the five cytokines was pipetted into the downstream reservoir (port 6). This sample was then electroosmotically transported into the entire fluidic network by applying 50 V to reservoir 6 and electrically grounding the upstream reservoirs for about 3 min. Following this step, the sample was incubated against the channel surface under stagnant conditions for 1 h and later washed out of the fluidic network with a phosphate buffer wash. The assay surface was finally completed by reacting with the 0.2-µg/ml solution of streptavidin-conjugated alkaline phosphatase as before. Additionally, we also prepared a device to quantitate the blank assays for the five cytokines following the same procedure as outlined for the multiplex unit except for replacing the sample solution with the sample diluent. In order to reference the performance of our multiplex device, we repeated the calibration and blank ELISAs in individual straight channels following procedures as described in our previous works [30, 31]. Because these channels were entirely coated with the same reagent during an incubation step, we only relied on using vacuum to draw the solution into the conduit that then was incubated against the channel surface under stagnant conditions.

2.3 | Device operation

The ELISAs were performed by reacting a solution containing 1-mM 4-methylumbelliferyl phosphate (4-MUP) and 1-mM $MgCl_2$ prepared in a 0.1-M sodium tetraborate buffer (pH 9.2) against the assay surface. 4-MUP is converted into 4-methylumbelliferyl by alkaline phosphatase during the course of the enzyme reaction. For our assays, the 4-MUP solution was introduced into an empty fluidic network using capillary forces with no fluid reservoirs attached to the channel terminals. The minimal amount of liquid at the channel ports ensured the no-flow condition needed within the conduits to prevent any advective transport of the enzyme reaction product across the adjacent ELISA segments in the multiplex device. The drying of the liquid from the channel terminals during the enzyme reaction period was minimized by sealing them with adhesive tapes. The ELISA reaction was performed at 37°C by placing the device close to a heating fan. Fluorescence measurements at the center of each ELISA region were made using an epifluorescence microscope (Nikon) with

bandpass excitation (380–391 nm) and emission (420–480 nm) optical filters. The fluorescence image thus obtained was recorded using a CCD camera (Roper Scientific) and analyzed with the Adobe Photoshop software. To minimize any unwanted signal generation in our system through photooxidation of the enzyme substrate, the ELISA regions were exposed to the excitation beam for about 1 s during the imaging process through the use of a mechanical shutter. The camera exposure time was set to 100 ms and the neutral density filters (ND8 and ND4) were engaged during the fluorescence measurements. The images thus obtained were analyzed using the Adobe Photoshop software.

3 | RESULTS AND DISCUSSION

3.1 | Flow simulation and visualization

In order to characterize the EOF in our microchip device during selective coating of the different assay segments, the distribution of the electric voltage was numerically solved for using the Partial Differential Equation toolbox in MATLAB. Figure 1B shows this distribution when 1 V is applied at the upstream reservoirs (ports 1–5 in Figure 1A) while electrically grounding the downstream one (port 6 in Figure 1A). The simulations show that when our fluidic network is chosen to be uniformly deep and wide as was the case for the devices used in this work, the electrical current, electric field and therefore the EOF, in the straight channel segments are twice in magnitude compared to those in the curved ones. For an applied voltage-drop of 50 V across the upstream and downstream reservoirs, this pattern yields an electric field just under 25 and 50 V/cm in the curved and straight regions of the channel layout. The EOF realized under these conditions was visualized by flowing in a dye (rhodamine B) solution and a dye-free buffer from reservoirs 1 and 2, respectively, as is shown in the image included Figure 1A. Flow velocities of about 50 and 100 μm/s were estimated in the curved and straight sections of the microchip based on these visualizations, which corresponded to drawing less than 6 μl of liquid from the upstream reservoirs over a 1-h coating period.

3.2 | Calibration experiments

All ELISAs performed during the current study were quantitated following the kinetic format of the assay as it yielded a more reliable approach to estimating the analyte concentration [32]. In this format, images of the assay channel were taken at multiple points in time over a 40-min enzyme reaction period from which the fluorescence intensities were later extracted. For the multiplex device, these images were taken at the center of each assay segment to minimize interference from its neighboring regions. The recorded intensities were then plotted against the enzyme reaction time for the various concentrations of the different cytokines considered in this work. In Figure 2, we have presented this experimental data showing a linear relationship between the two quantities with the slope of the line increasing for larger cytokine concentrations. However, the background fluorescence in the assay regions varied irregularly yielding an y-intercept for these curves that somewhat obscured the noted trend in the slopes. In order to reference these results, we repeated the calibration experiments in individual straight channels that again produced similar outcomes (see Figure 3). In this situation, the slopes of the best fitted lines from Figures 2 and 3 were plotted against the concentration of the cytokines (see Figure 4). As may be seen, the observed variation in these slopes with the cytokine concentration was reasonably described by a straight line providing us with the calibration curves for our multiplex assay. Notice that the standard deviation in the estimated slopes for a majority of the fitted lines included in Figure 4 was less than 0.01 a.u./min. In this situation, the lowest concentration for each of the cytokines was chosen such that it produced an assay signal of about 0.02–0.03 a.u./min that would correspond to the detection limit for that molecular species. Any lower analyte concentration was not considered for our experiments as that would have produced unreliable data. The higher concentrations for the calibration curve were picked by successively doubling this lowest value. In any case, once the functionality of our multiplex device was established, we proceeded to quantitate the concentrations of all five cytokines simultaneously in a standard sample based on the calibration curves included in Figure 4.

3.3 | Multiplex assays

It is important to point out that the calibration curves included in Figure 4 generated with standard samples containing a single cytokine species may only be applied to our multiplex assay provided that the cross-reactivity in our system is insignificant. To determine the validity of this assumption, a sample containing known concentrations of the five cytokines was prepared and introduced into our multiplex device. The center of each assay segment was subsequently imaged over the enzyme reaction period to quantitate the sample. In Figure 5A, we have presented the fluorescence signal thus recorded, which is seen to increase linearly with the enzyme reaction time as expected. This temporal rate of increase in the fluorescence signal was then mapped against the calibration

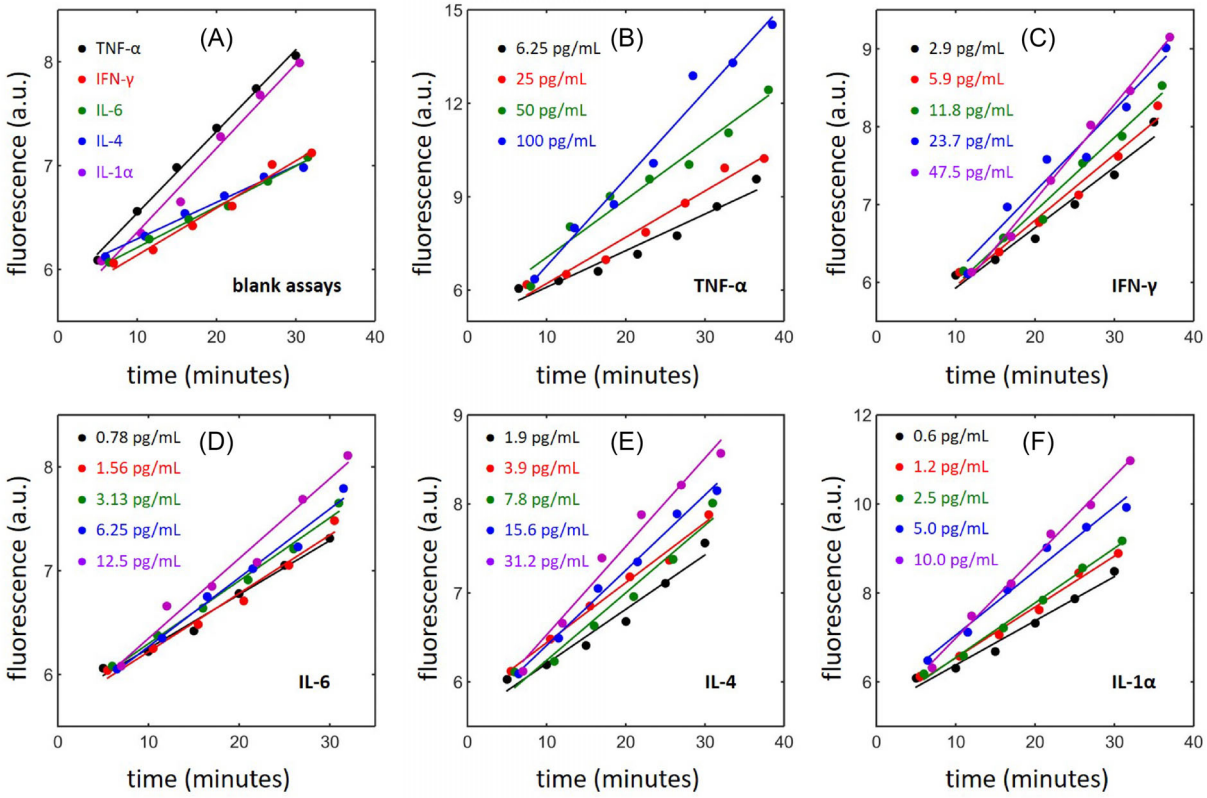

FIGURE 2 Temporal variation in the observed fluorescence signal recorded when analyzing standard (A) blank, (B) TNF-α, (C) IFN-γ, (D) IL-6, (E) IL-4 and (F) IL-1α samples using the multiplex device

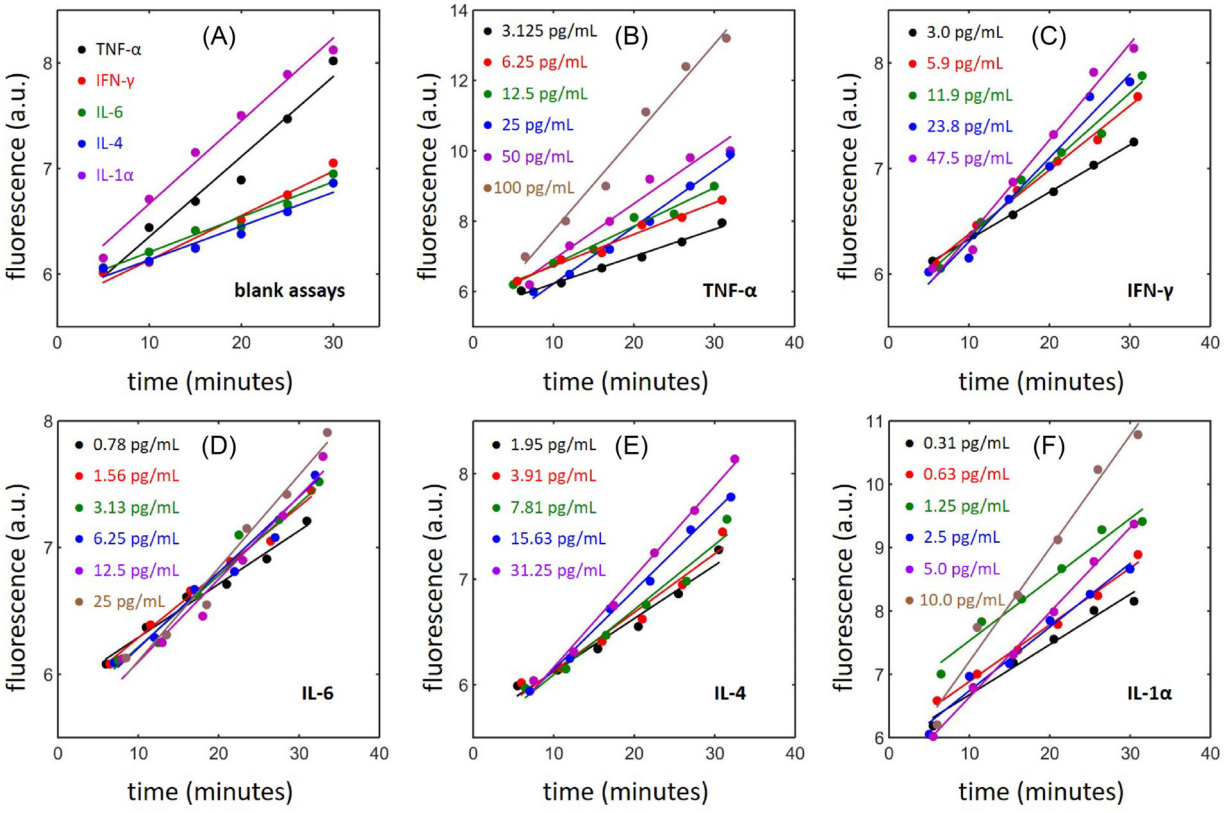

FIGURE 3 Temporal variation in the observed fluorescence signal recorded when analyzing standard (A) blank, (B) TNF-α, (C) IFN-γ, (D) IL-6, (E) IL-4 and (F) IL-1α samples in individual straight channels

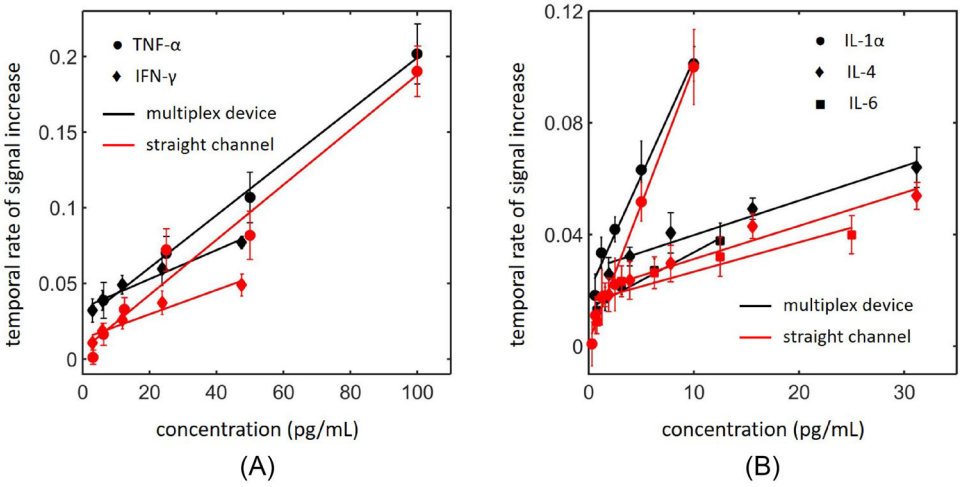

FIGURE 4 Calibration curves generated with the multiplex device and individual straight channels for the standard (A) TNF-α, IFN-γ and (B) IL-1α, IL-4, IL-6 samples.

(A)

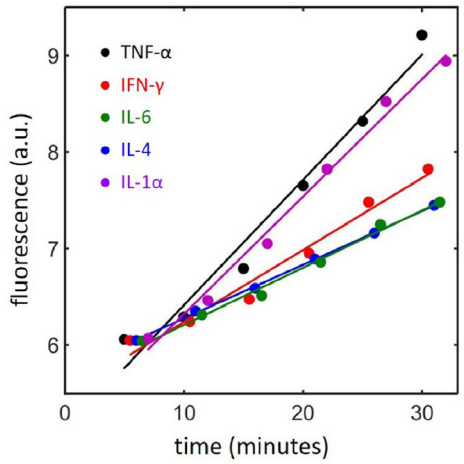

(B)

cytokine	actual concentration (pg/mL)	estimated concentration with the calibration curves generated using the multiplex device (pg/mL)	estimated concentration with the calibration curves generated using the straight channels (pg/mL)
TNF-α	25.0	26.5	24.3
IFN-γ	23.7	21.9	22.8
IL-6	3.1	2.8	2.9
IL-4	7.8	6.6	7.1
IL-1α	5.0	4.2	4.7

FIGURE 5 (A) Fluorescence measurements made for the multiplex assay. (B) Comparison of the actual and estimated concentrations in the cytokine sample as determined based on the calibration curves generated using the multiplex and straight channel devices

curves included in Figure 2 to back calculate the cytokine concentration in our standard sample. In Figure 5B, the cytokine concentrations thus estimated were compared to their actual values, which shows a deviation by less than 20% in all cases. Interestingly, upon reestimating these concentrations based on the calibration curves generated using the straight channels (Figure 3), the noted deviation is cut down to less than 10% indicating our multiplex device to be somewhat more error prone than the single channel setup.

Although the observed error in our multiplex measurements could not be reduced with our current experimental design, we nevertheless identified two major sources for it. First, the mechanical vibration of the microscope stage, where the microchip was placed during the enzyme reaction period, was seen to cause small oscillations in the fluid position within the channel network. Such oscillatory flows likely produced the waviness recorded in some of the curves included in Figures 2, 3 and 5A increasing the magnitude of error in their slopes. The oscillatory fluid motion was observed in our setup by introducing a rhodamine B solution into an assay segment such that it occupied only a fraction of the segment. The interface of this solution with the dye-free buffer was then monitored over time scales similar to the enzyme reaction period, which suggested an amplitude and frequency on the orders of 1 mm and 0.01 Hz, respectively, for the noted oscillatory motion. The accuracy of these measurements, however, was compromised by the diffusion of the dye molecules across the interface. Another major source of error in our measurements originated from the variability in the background fluorescence recorded for the different assay segments as has been pointed out in the previous section. Again, although the exact reason for this variation is unclear to us, it likely resulted from the inconsistencies in our microchip fabrication and channel derivatization processes. The two sources of error identified abovepossibly introduced some of the anomalous behavior seen in the temporal profile for the fluorescence signal included in Figures 2, 3 and 5A. However, their influence on the slope of these profiles was moderate allowing us to reasonably quantitate the assays described in this work. Nevertheless, we plan to explore the possibility of minimizing these errors in future works

by isolating our device from the mechanical vibrations, reducing the channel depth to increase their hydrodynamic resistance and minimize the oscillatory flows as well as adopting the use of polymer microchips that can be produced following simpler and more standardized procedures.

4 | CONCLUDING REMARKS

To conclude, microfluidic networks present a promising avenue for miniaturizing multiplex ELISAs by exploiting the slow diffusion of the enzyme reaction product across the assay regions. In this work, we have demonstrated a 5-plex cytokine ELISA based on this central idea using 1 μl of a sample in a fluidic network patterned over a $1.5 \times 1.5\text{-cm}^2$ region. The concentrations estimated from this assay matched within 20% of their actual values based on calibration curves that were again generated using a similar multiplex device. The current work also demonstrates that selective patterning of the assay segments with different antibodies/antigens may be easily realized using EOF in the reported device. In fact, this flow mode was found to offer a better control over the liquid velocities compared to pressure-drive that can improve the reliability of our assays as well as cut down the volume of the antibody/antigen solution required for the pattering process. Additionally, the use of EOF mode simplifies the instrumentation needs and can allow further miniaturization of the channel cross-sectional dimensions bringing down the sample volume requirement for our multiplex assays even further.

ACKNOWLEDGMENTS

This research work was supported by funds from the National Science Foundation and Wyoming INBRE program through grants CHE-1808507 and P20GM103432, respectively.

CONFLICT OF INTEREST

The authors have declared no conflict of interest.

DATA AVAILABILITY STATEMENT

The data that support the findings of this study are available from the corresponding author upon reasonable request.

ORCID

Debashis Dutta https://orcid.org/0000-0003-0938-3151

REFERENCES

1. Wild D. The immunoassay handbook. 4th ed. Oxford: Elsevier; 2013.
2. Kemeny DM, Challacombe SJ. ELISA and other solid phase immunoassays: theoretical and practical aspects. New York: John Wiley & Sons; 1988.
3. Edwards R. Immunoassay: an introduction. London: William Heinemann Medical Books; 1985.
4. Ngo TT. Electrochemical sensors in immunological analysis. New York: Plenum Press; 1987.
5. Price CP, Newman DJ. Principles and practice of immunoassay. 2nd ed. New York: Stockton Press; 1997.
6. Kanda V, Kariuki JK, Harrison DJ, Mcdermott MT. Label-free reading of microarray-based immunoassays with surface plasmon resonance imaging. Anal Chem. 2004;76:7257–62.
7. Terry LA, White SF, Tigwell LJ. The application of biosensors to fresh produce and the wider food industry. J Agric Food Chem. 2005;53:1309–16.
8. Zangar RC, Varnum SM, Bollinger N. Studying cellular processes and detecting disease with protein microarrays. Drug Metab Rev. 2005;37:473–87.
9. Jung Y, Jeong JY, Chung BH. Recent advances in immobilization methods of antibodies on solid supports. Analyst. 2008;133:697–701.
10. Crowther JR. ELISA: theory and practice. Methods Mol Biol. 1995;42:1–218.
11. Morgan CL, Newman DJ, Price CP. Immunosensors: technology and opportunities in laboratory medicine. Clin Chem. 1996;42:193–209.
12. Hartmann M, Roeraade J, Stoll D, Templin MF, Joos TO. Protein microarrays for diagnostic assays. Anal Bioanal Chem. 2009;393:1407–16.
13. Cheng C-M, Martinez AW, Gong J, Mace CR, Phillips ST, Carrilho E, et al. Paper-based ELISA. Angew Chem Int Ed Engl. 2010;49:4771–4.
14. Hu J, Wang S, Wang L, Li F, Pingguan-Murphy B, Lu TJ, et al. Advances in paper-based point-of-care diagnostics. Biosens Bioelectron. 2014;54:585–97.
15. Shen Li, Hagen JA, Papautsky I. Point-of-care colorimetric detection with a smartphone. Lab Chip. 2012;12:4240–3.
16. Yanagisawa N, Mahmud S, Dutta D. Absorbance detection in multireflection microfluidic channels using a commercial microplate reader system. Anal Chem. 2020;92:13050–7.
17. Chen Si, Svedendahl M, Van Duyne RP, Käll M. Plasmon-enhanced colorimetric ELISA with single molecule sensitivity. Nano Lett. 2011;11:1826–30.
18. Cohen L, Walt DR. Single-molecule arrays for protein and nucleic acid analysis. Annu Rev Anal Chem (Palo Alto Calif). 2017;10:345–63.
19. Cohen L, Cui N, Cai Y, Garden PM, Li X, Weitz DA, et al. Single molecule protein detection with attomolar sensitivity using droplet digital enzyme-linked immunosorbent assay. ACS Nano. 2020;14:9491–501.
20. Yanagisawa N, Mecham JO, Corcoran RC, Dutta D. Multiplex ELISA in a single microfluidic channel. Anal Bioanal Chem. 2011;401:1173–81.
21. Wang HY, Foote RS, Jacobson SC, Schneibel JH, Ramsey JM. Low temperature bonding for microfabrication of chemical analysis devices. Sens Actuators B. 1997;45:199–207.
22. Ermakov SV, Jacobson SC, Ramsey JM. Computer simulations of electrokinetic injection techniques in microfluidic devices. Anal Chem. 2000;72:3512–7.

23. Székely L, Guttman A. New advances in microchip fabrication for electrochromatography. Electrophoresis. 2005;26:4590–4.
24. Xia L, Dutta D. Microfluidic flow counterbalanced capillary electrophoresis. Analyst. 2013;138:2126–33.
25. Probstein RF. Physicochemical hydrodynamics. 2nd ed. New York: John Wiley & Sons; 1994.
26. Hu G, Gao Y, Sherman PM, Li D. A microfluidic chip for heterogeneous immunoassay using electrokinetical control. Microfluid Nanofluid. 2005;1:346–55.
27. Dodge A, Fluri K, Verpoorte E, De Rooij NF. Electrokinetically driven microfluidic chips with surface-modified chambers for heterogeneous immunoassays. Anal Chem. 2001;73:3400–9.
28. Giri B, Dutta D. Improvement in the sensitivity of microfluidic ELISA through field amplified stacking of the enzyme reaction product. Anal Chim Acta. 2014;810:32–8.
29. Giri B, Liu Y, Nchocho FN, Corcoran RC, Dutta D. Microfluidic ELISA employing an enzyme substrate and product species with similar detection properties. Analyst. 2018;143:989–98.
30. Pena J, Mcallister SJ, Dutta D. A glass microchip device for conducting serological survey of West Nile viral antibodies. Biomed Microdevices. 2014;16:737–43.
31. Giri B, Peesara RR, Yanagisawa N, Dutta D. Undergraduate laboratory module for implementing ELISA on the high performance microfluidic platform. J Chem Educ. 2015;92:728–32.
32. Yanagisawa N, Dutta D. Kinetic ELISA in microfluidic channels. Biosensors. 2011;1:58–69.

How to cite this article: Giri B, Dutta D. A compact microfluidic geometry for multiplexing enzyme-linked immunosorbent assays. Electrophoresis. 2022;43:1399–1407. https://doi.org/10.1002/elps.202100311